

This work was written as part of one of the author's official duties as an Employee of the United States Government and is therefore a work of the United States Government. In accordance with 17 U.S.C. 105, no copyright protection is available for such works under U.S. Law.

Public Domain Mark 1.0

<https://creativecommons.org/publicdomain/mark/1.0/>

Access to this work was provided by the University of Maryland, Baltimore County (UMBC) ScholarWorks@UMBC digital repository on the Maryland Shared Open Access (MD-SOAR) platform.

**Please provide feedback**

Please support the ScholarWorks@UMBC repository by emailing [scholarworks-group@umbc.edu](mailto:scholarworks-group@umbc.edu) and telling us what having access to this work means to you and why it's important to you. Thank you.

# PCCP

Physical Chemistry Chemical Physics

This paper is published as part of a PCCP Themed Issue on:

## Nanophotonics: Plasmonics and Metal Nanoparticles

Guest Editors: Greg V. Hartland (University of Notre Dame) and Paul Mulvaney (University of Melbourne)

### Editorial

#### Nanophotonics: plasmonics and metal nanoparticles

*Phys. Chem. Chem. Phys.*, 2009

DOI: [10.1039/b911746f](https://doi.org/10.1039/b911746f)

### Communication

#### Recombination rates for single colloidal quantum dots near a smooth metal film

Xiaohua Wu, Yugang Sun and Matthew Pelton, *Phys. Chem. Chem. Phys.*, 2009

DOI: [10.1039/b903053k](https://doi.org/10.1039/b903053k)

### Papers

#### Gain and loss of propagating electromagnetic wave along a hollow silver nanorod

Haining Wang and Shengli Zou, *Phys. Chem. Chem. Phys.*, 2009

DOI: [10.1039/b901983a](https://doi.org/10.1039/b901983a)

#### Two-photon imaging of localized optical fields in the vicinity of silver nanowires using a scanning near-field optical microscope

Kohei Imura, Young Chae Kim, Seongyong Kim, Dae Hong Jeong and Hiromi Okamoto, *Phys. Chem. Chem. Phys.*, 2009

DOI: [10.1039/b904013g](https://doi.org/10.1039/b904013g)

#### Anisotropy effects on the time-resolved spectroscopy of the acoustic vibrations of nanoobjects

Aurélien Crut, Paolo Maioli, Natalia Del Fatti and Fabrice Vallée, *Phys. Chem. Chem. Phys.*, 2009

DOI: [10.1039/b902107h](https://doi.org/10.1039/b902107h)

#### Coupling to light, and transport and dissipation of energy in silver nanowires

Hristina Staleva, Sara E. Skrabalak, Christopher R. Carey, Thomas Kosel, Younan Xia and Gregory V. Hartland, *Phys. Chem. Chem. Phys.*, 2009

DOI: [10.1039/b901105f](https://doi.org/10.1039/b901105f)

#### The versatile colour gamut of coatings of plasmonic metal nanoparticles

Catherine S. Kealley, Michael B. Cortie, Abbas I. Maarof and Xiaoda Xu, *Phys. Chem. Chem. Phys.*, 2009

DOI: [10.1039/b903318a](https://doi.org/10.1039/b903318a)

#### Probing the surface-enhanced Raman scattering properties of Au–Ag nanocages at two different excitation wavelengths

Matthew Rycenga, Kirk K. Hou, Claire M. Copley, Andrea G. Schwartz, Pedro H. C. Camargo and Younan Xia, *Phys. Chem. Chem. Phys.*, 2009

DOI: [10.1039/b903533h](https://doi.org/10.1039/b903533h)

#### The effect of surface roughness on the plasmonic response of individual sub-micron gold spheres

Jessica Rodríguez-Fernández, Alison M. Funston, Jorge Pérez-Juste, Ramón A. Álvarez-Puebla, Luis M. Liz-Marzán and Paul Mulvaney, *Phys. Chem. Chem. Phys.*, 2009

DOI: [10.1039/b905200n](https://doi.org/10.1039/b905200n)

#### White light scattering spectroscopy and electron microscopy of laser induced melting in single gold nanorods

Peter Zijlstra, James W. M. Chon and Min Gu, *Phys. Chem. Chem. Phys.*, 2009

DOI: [10.1039/b905203h](https://doi.org/10.1039/b905203h)

#### Influence of the close sphere interaction on the surface plasmon resonance absorption peak

Carlos Pecharromán, *Phys. Chem. Chem. Phys.*, 2009

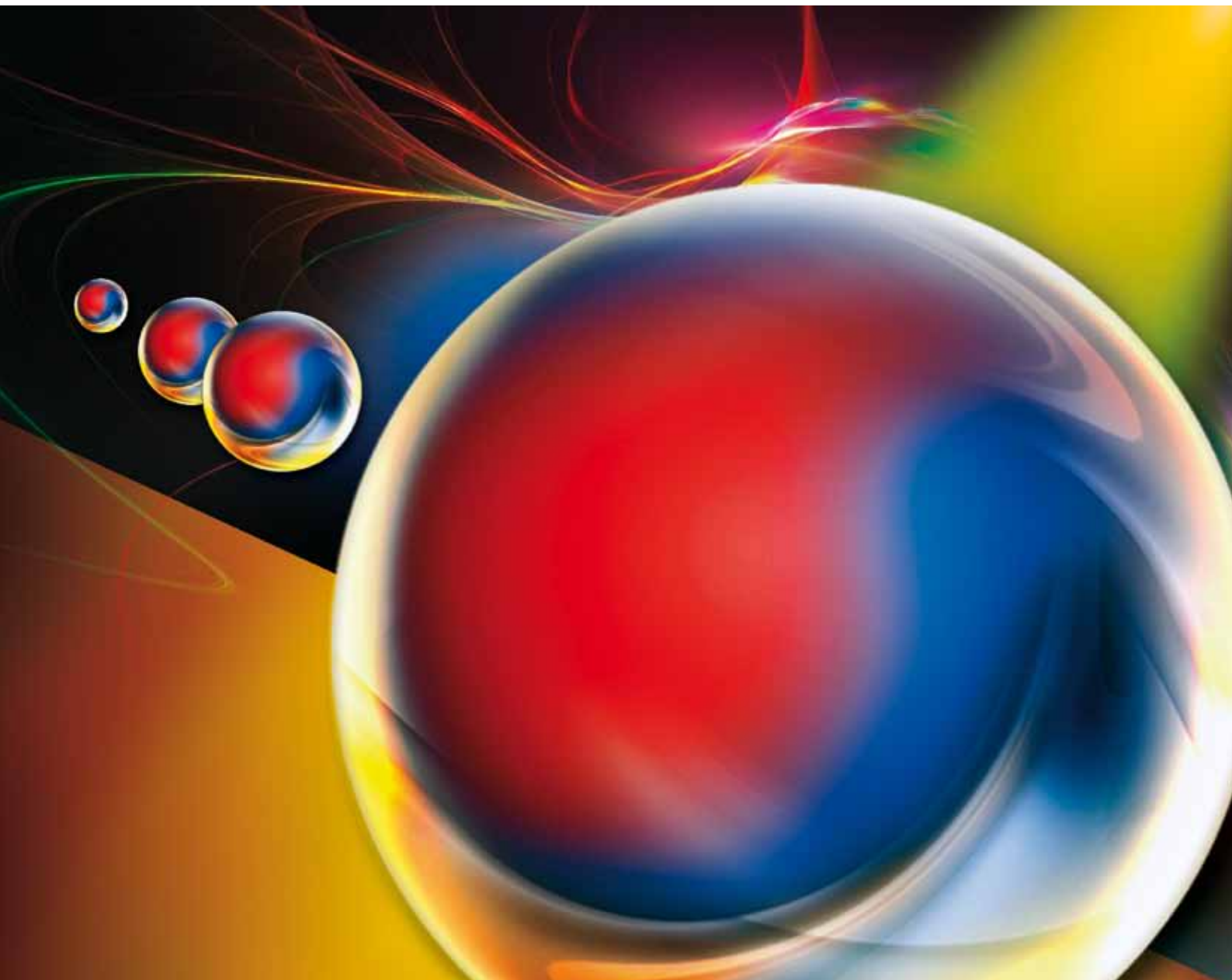
DOI: [10.1039/b902489c](https://doi.org/10.1039/b902489c)

# PCCP

Physical Chemistry Chemical Physics

[www.rsc.org/pccp](http://www.rsc.org/pccp)

Volume 11 | Number 28 | 28 July 2009 | Pages 5853–6016



Includes a collection of articles on the theme of Nanophotonics: Plasmonics and Metal Nanoparticles

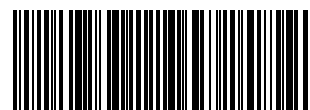
ISSN 1463-9076

**COVER ARTICLE**

Pelton and Wu  
Recombination rates for single colloidal  
quantum dots near a smooth metal film

**HOT ARTICLE**

Liz-Marzán *et al.*  
Effect of surface roughness on  
plasmonic response of sub-micron  
gold spheres



1463-9076(2009)11:28;1-T

# Recombination rates for single colloidal quantum dots near a smooth metal film†

Xiaohua Wu, Yugang Sun and Matthew Pelton\*

Received 13th February 2009, Accepted 21st May 2009

First published as an Advance Article on the web 5th June 2009

DOI: 10.1039/b903053k

**This paper presents experimental distributions of recombination rates for excitons in individual CdSe–ZnS core–shell quantum dots separated from a smooth gold film by a nanometre-scale dielectric layer. By measuring emission kinetics as a function of time, we obtain intrinsic recombination rates for single quantum dots. The distribution of recombination rates broadens and its maximum value increases as the separation between the dots and the metal decreases. The results agree with a semiclassical model that takes into account the randomly oriented two-dimensional dipole moments of the quantum dots.**

When an optical emitter is placed in nanometre-scale proximity to a metal structure, its emission properties can be strongly modified due to coupling between the emitter and excitations in the metal, particularly surface plasmons. This phenomenon has recently attracted considerable attention, both for the development of a basic understanding of nano-scale photophysics and for potential applications.<sup>1,2</sup> In particular, metal-enhanced emission has the potential to improve the performance of light-emitting devices, to compensate losses in plasmonic devices, and to lead to novel phenomena such as surface-plasmon lasing. Colloidal semiconductor nanocrystals, or quantum dots (QDs), are particularly promising for such applications, due to their large dipole moments and photostability. So far, most experimental studies of QD–metal interactions have considered only changes in fluorescence intensity. In this case, though, several competing mechanisms contribute to the measured signal, including enhanced absorption of the excitation light, changes in the spatial pattern of emission, and changes in radiative and non-radiative recombination rates. The recombination rates provide the most direct measure of the QD–metal coupling, and have been directly investigated for ensembles of QDs near smooth metal films or metal nanostructure arrays.<sup>3–5</sup> A smooth film is the simplest metal structure capable of modifying QD emission, and thus presents an ideal model for understanding the underlying physical phenomena. In the ensemble, though, QD emission is inhomogeneously

broadened and recombination kinetics are highly non-exponential, making it difficult to extract meaningful decay rates. Other studies have probed single QDs on rough metal films;<sup>6,7</sup> in this case, though, each QD is surrounded by a unique and unknown nanostructured metal environment, and quantitative understanding is again difficult to obtain.

In this communication, we present results of measurements of recombination kinetics of excitons in individual QDs near smooth gold films. We find that temporal fluctuations in QD recombination rates obscure the effects of the metal coupling, which can therefore be isolated only by resolving the recombination kinetics in time. We vary the distance,  $d$ , between the QD and the metal, and collect recombination-rate distributions by repeating measurements on several different dots. We find that as  $d$  decreases, the distributions broaden and their maximum value increases. The increase in the maximum recombination rate is caused by energy transfer from the QD exciton to the gold film. The broadening of the distribution, on the other hand, is due to inherent variations in the interaction between the gold film and individual QDs with different crystal orientations. These effects are confirmed by quantitatively comparing the experimental results to a simple semiclassical model.

Fig. 1 shows a simple sketch of the sample structure and the fluorescence measurement setup. The samples are prepared as follows. First, a diluted solution of CdSe–ZnS core–shell QDs (Evident Technologies Evidot) is spin cast onto a clean glass coverslip (FisherSci, refractive index = 1.52), producing a sparse layer of isolated dots with an areal density of about 1 per 10  $\mu\text{m}^2$ . Second, a polymethyl methacrylate (PMMA, MicroChem 950PMMA A, refractive index = 1.48) layer is spin-coated on top of the QD layer, and the sample is

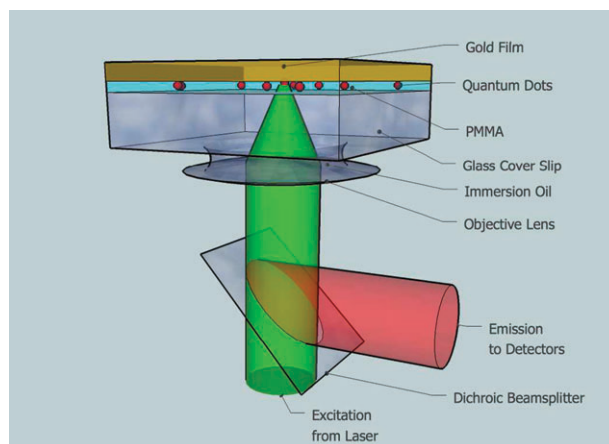


**Fig. 1** Schematic of the sample structure and the experimental setup.

Center for Nanoscale Materials, Argonne National Laboratory,  
9700 South Cass Avenue, Argonne, IL 60439, USA.  
E-mail: pelton@anl.gov

† The submitted manuscript has been created by UChicago Argonne, LLC, Operator of Argonne National Laboratory (Argonne). Argonne, a US Department of Energy Office of Science laboratory, is operated under Contract No. DE-AC02-06CH11357. The US Government retains for itself, and others acting on its behalf, a paid-up nonexclusive, irrevocable worldwide license in said article to reproduce, prepare derivative works, distribute copies to the public, and perform publicly and display publicly, by or on behalf of the Government.

baked on a hotplate at 140 °C for 5 min. The thickness of the PMMA layer determines the separation,  $d$ , between the dots and the metal, and is controlled by selecting the solution concentration and the spin speed. Finally, a 100 nm gold film is deposited onto the PMMA layer by electron-beam evaporation ( $0.5 \text{ nm s}^{-1}$ , base pressure =  $10^{-6}$  Torr). Prior to the metal deposition, the roughness of the PMMA layer is determined by atomic force microscopy to be less than 2 nm. Optical emission from the QDs is measured at room temperature in an *epi*-fluorescence configuration. The dots are excited by frequency-doubled pulses from a mode-locked Ti:sapphire laser (400 nm excitation wavelength, 5 MHz repetition rate). The excitation beam is focused onto a single QD through the coverslip by a 60X /1.4 N.A. oil-immersion objective, and the same lens is used to collect the emission. The emission is separated from reflected laser light with a dichroic mirror and two bandpass filters, and is then detected by a single-photon counter (Micro Photon Devices PDM). Output pulses from the detector are sent to the input channel of a time-correlated single-photon counting (TCSPC) module (PicoQuant PicoHarp 300). Sync pulses from the Ti:sapphire laser are sent to the other input channel of this TCSPC module, which can thus record the arrival time of every photon relative to the start of the experiment as well as the time delay,  $\tau_p$ , between each detected photon and the preceding sync pulse. Together, the detector and the TCSPC module provide a timing resolution of approximately 50 ps.

An intensity trajectory,  $I(t)$ , is generated by dividing the duration of the experiment into 10 ms time bins and counting the number of photons that arrive within each bin. Fig. 2(a) shows part of a typical trajectory for a QD in a sample with  $d = 20 \text{ nm}$ . The intensity exhibits large fluctuations, or “blinking”, characteristic of fluorescence from single QDs.<sup>8</sup> Previous measurements have demonstrated that the fluctuations in intensity are accompanied by changes in recombination rates.<sup>9</sup> Lower intensities correspond to faster decay rates, suggesting that the blinking behavior is due to fluctuations in non-radiative recombination rates. When the emission intensity is at its maximum, the recombination is well described by a single exponential; moreover, the decay rate in this maximum-intensity state is nearly identical across different dots and different samples. It was therefore proposed that the “maximum-intensity” decay rate,  $\gamma_m$ , corresponds to the radiative recombination rate of the QD. Based on this result, we extract  $\gamma_m$  for individual quantum dots near a metal film, thereby determining intrinsic recombination rates that are independent of fluctuating non-radiative processes. When the metal film is present, this intrinsic recombination rate includes not only radiative decay to the environment but also non-radiative energy transfer to the metal. Here, we do not treat these two processes separately, but study instead the total change in recombination rate as the QD approaches the metal film.

Fig. 2(b) illustrates our data-analysis method. A histogram of  $\tau_p$  for all the detected photons shows a highly multi-exponential decay, reflecting the large temporal fluctuations in recombination rates. In order to isolate the photons emitted when the dot is in its maximum-intensity state, we set a threshold in the emission-intensity trajectory at 70% of the difference between

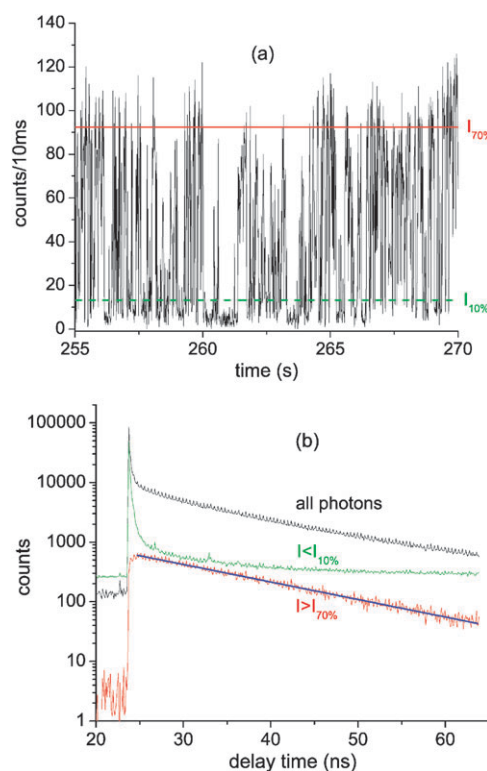


**Fig. 2** (a) Part of an emission-intensity trajectory for a quantum dot 20 nm away from a smooth gold film. Photon counts are grouped into 10 ms time bins. The two horizontal lines show threshold intensities at 70% (solid) and 10% (dashed) of the difference between the maximum and minimum emission intensities. (b) Histogram of photon counts as a function of delay time,  $\tau_p$ , after excitation laser pulse. Results are shown for all photons, for  $I < I_{10\%}$  (offset by 200 in  $y$  for clarity), and for  $I > I_{70\%}$ . The straight line is a fit to a single exponential, which yields the maximum-intensity decay rate  $\gamma_m = 0.068 \text{ ns}^{-1}$ .

the maximum and minimum measured intensities (illustrated in Fig. 2(a)); *i.e.* the threshold is at  $I_{70\%} = I_{\min} + 0.7(I_{\max} - I_{\min})$ , where  $I_{\min}$  is the minimum value of  $I(t)$  and  $I_{\max}$  is the maximum value. The photons emitted when the intensity is above this threshold are then used to construct a new histogram of  $\tau_p$ . This histogram still contains a small background of photons emitted from the metal and the PMMA layers. In order to remove this background, we first collect another histogram of photons emitted when the intensity is below the threshold  $I_{10\%} = I_{\min} + 0.1(I_{\max} - I_{\min})$ , as shown in Fig. 2(b). The background decay curve is subtracted from the maximum-intensity decay curve after first normalizing by  $t_{70\%}/t_{10\%}$ , where  $t_{70\%}$  is the total amount of time for which  $I(t) > I_{70\%}$  and  $t_{10\%}$  is the total time for which  $I(t) < I_{10\%}$ . The resulting maximum-intensity decay curve is shown in Fig. 2(b), and can clearly be seen to decay according to a single exponential. Fitting the decay curve yields the intrinsic QD recombination rate,  $\gamma_m$ .

To study how the decay rate depends on the separation,  $d$ , between the QD and the metal, we repeat the entire process and determine  $\gamma_m$  for single QDs from a series of samples with different QD–metal separations  $d$ . In a control experiment, we measure  $\gamma_m$  for single QDs on a glass coverslip with a PMMA layer but no gold film. The resulting values of  $\gamma_m$ , shown in Fig. 3(a), follow a Gaussian distribution with a most probable



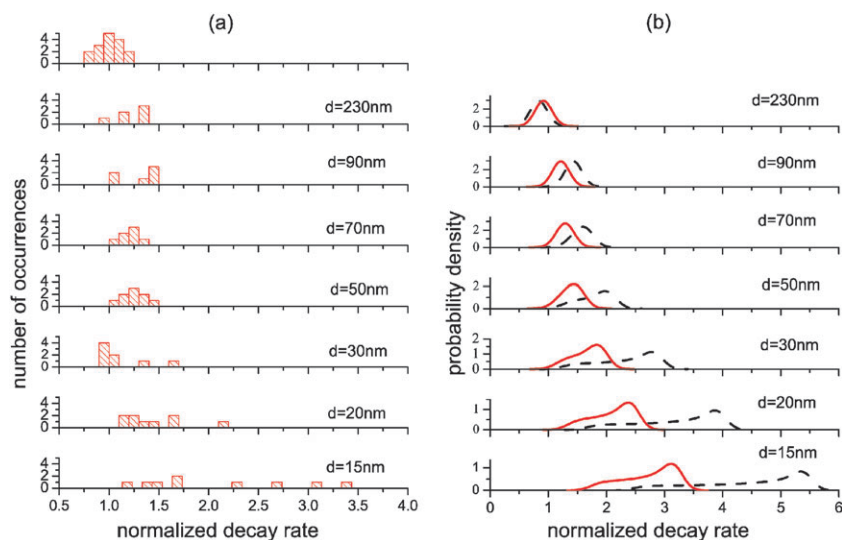


**Fig. 3** (a) Experimentally measured maximum-intensity decay rate  $\gamma_m$ . The top panel shows decay rates for quantum dots in the absence of a gold film; the most probable decay rate  $\gamma_{m0}$  from this histogram is used to normalize the data. The other panels show decay rates for dots at different distances  $d$  from a smooth gold film. (b) Calculated distribution,  $p(\gamma/\gamma_0)$ , of normalized decay rates. Results are shown for quantum yields,  $\Phi$ , of 0.5 (solid lines) and 1.0 (dashed lines).

value of  $\gamma_{m0} = 0.05 \text{ ns}^{-1}$ . We normalize  $\gamma_m$  for the QDs near metal films by  $\gamma_{m0}$  and plot the results in Fig. 3(a). It can be seen that, as  $d$  decreases, the  $\gamma_m$  distribution becomes broader and its average value increases. The increase in the mean decay rate is due to coupling between the QD and the metal film. This coupling is dependent on the orientation of the QD dipole and is significantly stronger for dipoles oriented normal to the surface of the metal film. The broadening of the decay-rate distribution thus reflects the random orientation of the dipoles of individual QDs.

In order to verify this interpretation of the measurement results, we calculate expected decay-rate distributions by considering a point dipole with arbitrary orientation in a multilayer structure. Such a model was first developed by Chance *et al.*<sup>10</sup> the same model was later developed mathematically in ref. 11, which we follow here. The radiation rates for a vertically-oriented dipole (normal to the surface of the metal film) and a horizontally-oriented dipole (along the surface of the metal film) are determined to be, respectively,

$$\frac{\gamma_v}{\gamma_0} = 1 - \Phi + \frac{3}{2} \Phi \operatorname{Re} \left[ \int_0^\infty \frac{u^3}{\sqrt{1-u^2}} (1 + \rho^{\text{TM}}(u)) du \right], \quad (1)$$

$$\begin{aligned} \frac{\gamma_h}{\gamma_0} = 1 - \Phi + \frac{3}{4} \Phi \operatorname{Re} \left[ \int_0^\infty \frac{u}{\sqrt{1-u^2}} ((1-u^2)(1 - \rho^{\text{TM}}(u)) \right. \\ \left. + (1 + \rho^{\text{TE}}(u)) du \right], \end{aligned} \quad (2)$$

where  $\gamma_0$  is the radiation rate for the dipole in vacuum,  $u = (k_{\parallel}\lambda)/(2\pi n)$  is the normalized transverse wave number (where  $n$  is the refractive index of the material surrounding the QDs),  $\Phi$  is the quantum yield of the emitting state, and  $\rho^{\text{TE}}(u)$  and  $\rho^{\text{TM}}(u)$  are the amplitude reflection coefficients for TE-polarized and TM-polarized waves, respectively. The reflection coefficients are calculated by taking into account the Fresnel reflections at the glass/PMMA and PMMA/gold interfaces; the glass coverslip and gold film are each assumed

to be thick enough that the other interfaces can be ignored. For the center QD emission wavelength of  $\lambda = 620 \text{ nm}$ , we use a refractive index of  $(0.21 + 3.272i)$  for gold.<sup>12</sup> A similar calculation gives  $\gamma \approx \gamma_0$  for all dipole orientations for the reference sample of QDs on a glass coverslip with PMMA but with no gold film; this justifies using this reference sample to normalize the experimental data.

The transition dipole of a CdSe QD is a two-dimensional superposition of the two orientations perpendicular to its crystalline  $c$  axis.<sup>13</sup> If the  $c$  axis is normal to the surface of the gold film, the recombination rate is simply  $\gamma_h$ ; if it is parallel to the surface, the recombination rate is  $(\gamma_h + \gamma_v)/2$ . In general, the  $c$  axis of a QD will be randomly oriented at an angle  $\theta$  to the normal, according to the distribution  $p(\theta) = \sin \theta$ , and will have a decay rate  $\gamma(\theta) = \gamma_h \cos^2 \theta + 1/2(\gamma_h + \gamma_v) \sin^2 \theta$ . By a change of variables, we obtain the decay-rate distribution

$$p(\gamma) = 1/\sqrt{(\gamma_v - \gamma_h)(\gamma_v + \gamma_h - 2\gamma)}. \quad (3)$$

This formula assumes a single lifetime for QDs in the absence of the metal film, and thus does not include the distribution of lifetimes due to variations among QDs in the ensemble. We take this intrinsic distribution into account by fitting a Gaussian to the measured distribution without the metal film and convolving this Gaussian with eqn (3); resulting theoretical distributions are shown in Fig. 3(b).

If we take the intrinsic quantum yield,  $\Phi$ , to be an adjustable parameter and set it equal to 0.5, we obtain distributions whose limits are in very good agreement with the experimental values. One feature in the theoretical distributions that is not observed experimentally is the increase in  $p(\gamma)$  with increasing  $\gamma$ . This can be explained by our tendency to measure emission from brighter dots: if a dot couples strongly to the film, so that  $\gamma/\gamma_0$  is large, then most of the energy is transferred to the metal and few photons can be detected. This experimental limitation becomes more serious as  $d$  decreases; in fact, for samples with  $d \leq 10 \text{ nm}$ , we cannot detect enough photons from any QD to

obtain an accurate value of  $\gamma_m$ . The bias toward brighter emitters is a universal difficulty in single-particle and single-molecule fluorescence measurements. A similar issue occurs in ensemble measurements, since the total signal measured is the weighted average of the signal from each dot, where the weighting is by the intensity of each dot's emission.

We note also that previous measurements have suggested that QDs typically have  $\Phi \approx 1$ , rather than the value of  $\Phi = 0.5$  that we assume here.<sup>9,14</sup> As shown in Fig. 3(b), setting  $\Phi = 1$  gives us much poorer agreement between theory and experiment. The discrepancy may be due to the relatively small number of QDs that can be measured in a reasonable amount of time and the unavoidable measurement bias towards brighter dots. In addition, the simple theory that we use ignores the variation in emission wavelength from dot to dot, the emission linewidth, the finite size of the quantum dots, and the presence of other electronic states in the dot apart from the emissive ground state. Nonetheless, the theory gives good qualitative agreement with experiment with only a single adjustable parameter for all the QD-metal separations, suggesting that it provides a useful understanding of the physical mechanisms underlying the optical interaction between QDs and a metal surface.

In summary, we have investigated the intrinsic recombination rates for single quantum dots in nanometre proximity to a smooth metal film. By making time-resolved measurements of decay kinetics, we removed the effects of non-radiative-rate fluctuations associated with blinking and determined intrinsic decay rates for a number of individual QDs. In agreement with theory, the measured decay-rate distributions broaden and shift to larger values as the dot-metal separation decreases. The results clearly demonstrate significant variations from dot to dot in the coupling to the metal due to the random orientation of the two-dimensional QD dipole. This simple

system thus provides an important framework that can be used to investigate the coupling of QDs to more complex metal structures. Any quantitative characterization of QD-metal coupling will require going beyond ensemble averaging and time averaging and making time-resolved kinetic measurements on individual quantum dots.

Work at the Center for Nanoscale Materials was supported by the US Department of Energy, Office of Science, Office of Basic Energy Sciences, under Contract No. DE-AC02-06CH1135. We thank Dr David Gosztola for help with the optical experiment.

## References

- 1 M. Pelton, J. Aizpurua and B. Garnett, *Laser Photonics Rev.*, 2008, **2**, 136, and references therein.
- 2 Y. Fu and J. R. Lakowicz, *Laser Photonics Rev.*, 2009, **3**, 221, and references therein.
- 3 K. Okamoto, S. Vaynashare and A. Scherer, *J. Opt. Soc. Am. B*, 2006, **23**, 1674.
- 4 A. Ueda, T. Tayagaki and Y. Kanemitsu, *Appl. Phys. Lett.*, 2008, **92**, 133118.
- 5 Y. Wang, T. Yang, M. T. Tuominen and M. Achermann, *Phys. Rev. Lett.*, 2009, **102**, 163001.
- 6 K. T. Shimizu, W. K. Woo, B. R. Fisher, H. J. Eisler and M. G. Bawendi, *Phys. Rev. Lett.*, 2002, **89**, 117401.
- 7 Y. Ito, K. Matsuda and Y. Kanemitsu, *Phys. Rev. B: Condens. Matter Mater. Phys.*, 2007, **75**, 033309.
- 8 P. Frantsuzov, M. Kuno, G. Janko and R. A. Marcus, *Nat. Phys.*, 2008, **4**, 519.
- 9 B. R. Fisher, H.-J. Eisler, N. E. Stott and M. G. Bawendi, *J. Phys. Chem. B*, 2004, **108**, 143.
- 10 R. R. Chance, A. Prock and R. Silbey, *J. Chem. Phys.*, 1974, **60**, 2744.
- 11 K. G. Sullivan and D. G. Hall, *J. Opt. Soc. Am. B*, 1997, **14**, 1149.
- 12 P. B. Johnson and R. W. Christy, *Phys. Rev. B: Condens. Matter Mater. Phys.*, 1972, **6**, 4370.
- 13 I. Chung, K. T. Shimizu and M. G. Bawendi, *Proc. Natl. Acad. Sci. U. S. A.*, 2003, **100**, 405.
- 14 X. Brokmann, L. Coolen, M. Dahan and J. P. Hermier, *Phys. Rev. Lett.*, 2004, **93**, 107403.